# The dynamics of fluorescently labeled endogenous *gurken* mRNA in *Drosophila*

**Angela M. Jaramillo[1,2], Timothy T. Weil[2], Joseph Goodhouse[2], Elizabeth R. Gavis[2] and Trudi Schupbach[1,2,*]**

[1]Howard Hughes Medical Institute and [2]Department of Molecular Biology, Princeton University, NJ 08544, USA

*Author for correspondence (e-mail: schupbac@princeton.edu)

*Accepted 11 December 2007*
*Journal of Cell Science 121, 887-894 Published by The Company of Biologists 2008*
*doi:10.1242/jcs.019091*

## Summary

**During *Drosophila* oogenesis, the targeted localization of *gurken* (*grk*) mRNA leads to the establishment of the axis polarity of the egg. In early stages of oogenesis, *grk* mRNA is found at the posterior of the oocyte, whereas in the later stages *grk* mRNA is positioned at the dorsal anterior corner of the oocyte. In order to visualize the real-time localization and anchorage of endogenous *grk* mRNA in living oocytes, we have utilized the MS2-MCP system. We show that MCP-GFP-tagged endogenous *grk* mRNA localizes properly within wild-type oocytes and behaves aberrantly in mutant backgrounds. Fluorescence recovery after photobleaching (FRAP) experiments of localized *grk* mRNA in egg chambers reveal a difference in the dynamics of *grk* mRNA between young and older egg chambers. *grk* mRNA particles, as a population, are highly dynamic molecules that steadily lose their dynamic nature as oogenesis progresses. This difference in dynamics is attenuated in *K10* and *sqd*$^{1}$ mutants such that mislocalized *grk* mRNA in older stages is much more dynamic compared with that in wild-type controls. By contrast, in flies with compromised dynein activity, properly localized *grk* mRNA is much more static. Taken together, we have observed the nature of localized *grk* mRNA in live oocytes and propose that its maintenance changes from a dynamic to a static process as oogenesis progresses.**

Supplementary material available online at
http://jcs.biologists.org/cgi/content/full/121/6/887/DC1

Key words: *grk*, Oogenesis, FRAP, RNA localization, *Drosophila*

## Introduction

Asymmetric messenger RNA localization provides a means to spatially restrict protein synthesis. In many cell types, on-site translation serves to maintain and elaborate a polarized architecture. However, the fundamental questions of how a transcript moves to its destination, how it remains translationally silent while in transit and how it is anchored at its target site remain unanswered for many mRNAs (reviewed in St Johnston, 2005). In *Drosophila*, several asymmetrically localized transcripts have been identified in the developing oocyte. *bicoid* mRNA is localized at the anterior of the oocyte, whereas *oskar* can be found spatially restricted at the posterior of the oocyte (Berleth et al., 1988; Ephrussi et al., 1991; Lehmann and Nusslein-Volhard, 1986). These transcripts, along with *gurken* (*grk*) mRNA, are necessary for the patterning of the *Drosophila* embryo. *gurken* encodes a transforming growth factor-α (TGFα)-like protein that is secreted by the oocyte and activates the epidermal growth factor receptor (EGFR) in the overlying somatic follicle cells. In early oogenesis, *grk* mRNA accumulates at the posterior of the oocyte. Gurken protein, synthesized from this RNA, induces posterior cell fates in the overlying follicle cells. Soon thereafter, during mid-to-late oogenesis, *grk* mRNA and protein are localized to the dorsal anterior corner of the oocyte, establishing dorsal cell fates in lateral follicle cells (Neuman-Silberberg and Schupbach, 1996; St Johnston, 2005; Van Buskirk and Schupbach, 1999).

Mutations in several genes have been identified that result in mislocalization of *grk* mRNA. Some of these genes, such as *squid* and *hrb27c*, encode heterogeneous nuclear ribonucleoproteins (hnRNPs) (Goodrich et al., 2004; Neuman-Silberberg and Schupbach, 1993), whereas others include genes necessary for cytoskeletal integrity, such as *cappuccino*, *spire* (an actin nucleator) and *spindle-F* (microtubule organizer) (Abdu et al., 2006; Manseau and Schupbach, 1989; Neuman-Silberberg and Schupbach, 1993). In addition, it has been shown that the motor enzymes kinesin and dynein are required for correct *grk* mRNA localization (Brendza et al., 2002; Clark et al., 2007; Delanoue et al., 2007; Duncan and Warrior, 2002; Januschke et al., 2002). These requirements suggest a model whereby *grk* mRNA is assembled into an RNP complex that is transported on filaments by molecular motors. In fact, *grk* mRNA synthesized in vitro and injected during mid-oogenesis assembles into nonmembranous transport particles that move first to the anterior of the oocyte and then dorsally towards the nucleus, and these movements are dependent on dynein. Furthermore, microtubule depolymerization disrupts the directionality of injected *grk* mRNA, implying active transport along microtubules (Clark et al., 2007; Delanoue et al., 2007; MacDougall et al., 2003). However, little is known about how *grk* mRNA is maintained or anchored at its destination. Recent ultrastructural analysis suggest that *grk* mRNA is not only transported but also anchored by dynein to large cytoplasmic structures called sponge bodies at the dorsal-anterior corner (Delanoue et al., 2007).

We have used a system for fluorescently labeling mRNA in vivo to visualize the real-time localization and anchoring of endogenous *grk* mRNA in living oocytes. We show that GFP-labeled endogenous *grk* mRNA properly localizes within wild-type oocytes and behaves aberrantly in mutant backgrounds. Interestingly, pharmacological studies show that the anchoring of *grk* mRNA might not be dependent on an intact cytoskeleton or, alternatively, it might utilize a subpopulation of microtubules that are very drug resistant. Fluorescence recovery after photobleaching (FRAP) experiments of *grk* mRNA particles in live egg chambers reveal a difference in the dynamic state of localized *grk* mRNA between early- and mid-stage egg chambers. *grk* mRNA particles, as a population, are highly dynamic molecules, exhibiting high fluorescence recovery, during

early stages. As oogenesis progresses, *grk* mRNA steadily loses its dynamic nature. This difference in *grk* mRNA mobility is attenuated in *K10* and *sqd*$^{1}$ mutants such that mislocalized *grk* mRNA in older stages remains much more dynamic. By contrast, in flies with compromised dynein activity, properly localized *grk* mRNA is more static. Taken together, we have observed the changing nature of localized *grk* mRNA in live oocytes and have demonstrated that its maintenance can be a dynamic process. We show that localized *grk* mRNA, as a population, can be highly dynamic or static, depending on the stage of oogenesis. Investigating the changing nature of *grk* mRNA allows us to gain insight into the mechanisms involved in the maintenance of localized transcripts.

## Results

### In vivo labeling of *gurken* mRNA in egg chambers

In order to visualize *grk* mRNA in live egg chambers, we took advantage of a system for fluorescent labeling of mRNA in vivo. We have utilized the MS2-MS2 coat protein (MS2-MCP) system pioneered by Singer and colleagues in yeast (Bertrand et al., 1998) and adapted for *Drosophila* by Gavis and colleagues (Forrest and Gavis, 2003; Weil et al., 2006). Twelve stem-loop binding sites for MCP were inserted into the 3′UTR of *grk* mRNA. The *grk-(MS2)*$_{12}$ transgene rescues the *grk*$^{2B}$ mutant phenotype, indicating that the stem loops do not significantly interfere with the function of the RNA. *grk-(MS2)*$_{12}$ was coexpressed with either the *hsp83-MCP-GFP* or the *hsp83-MCP-RFP* transgene, which encode MCP fused to either green fluorescent protein (GFP) or red fluorescent protein (RFP) (Weil et al., 2006). Eggs from flies expressing both transgenes, *grk-(MS2)*$_{12}$ together with *hsp83-MCP-GFP* or *hsp83-MCP-RFP* (referred to as *grk*GFP* and *grk*RFP*), show no obvious alterations in morphology. Moreover, the labeled RNAs, *grk*GFP* and *grk*RFP*, have localization patterns identical to that of wild-type *grk* mRNA.

As previously described, *grk* mRNA is expressed in early egg chambers (stages 1-7) and localized to the posterior end of the oocyte. Starting at stage 8, the oocyte nucleus moves from the center to the anterior edge of the oocyte. As the egg chamber grows, this edge will become the future dorsal anterior corner. During this stage, *grk* mRNA begins to accumulate around the new position of the nucleus as well as the anterior of the oocyte, creating a transient cortical ring. From stages 9 to 10B, *grk* mRNA remains in tight association with the dorsal anterior corner, forming a cap over the nucleus (Neuman-Silberberg and Schupbach, 1993). We used laser scanning confocal microscopy for live imaging of *grk*GFP* and *grk*RFP* during oogenesis (Fig. 1). Egg chambers were dissected and kept within a culture dish with nutrient media and then immediately imaged. Throughout early stages 4-7, *grk*GFP* and *grk*RFP* can be seen lining the posterior of the oocyte (Fig. 1A). During stage 7, when the oocyte nucleus is centered or shifting to one side, live images of *grk*GFP* show it to accumulate around the anterior cortex as well as continuing to line the posterior. At stage 8, the oocyte nucleus moves entirely to one side. As soon as the nucleus is asymmetric, the amount of *grk*GFP* at the posterior and ventral lateral sides of the oocyte decreases and, instead, *grk*GFP* appears to line the lateral wall posterior to the nucleus (Fig. 1B). At this stage, the dorsal-anterior cap of *grk*GFP* above the nucleus becomes increasingly prominent. While stage 8 progresses, *grk*GFP* continues to be visible anteriorly in a prominent ring, and meanwhile little to no *grk*GFP* can be seen at the posterior. As the egg chamber develops through stage 9, less and less *grk*RFP* accumulates in the ring, whereas *grk*RFP* in the ventral-anterior corner persists a bit longer, as previously reported by MacDougall and colleagues using fluorescent in situ hybridization (MacDougall et al., 2003). During this time, *grk*RFP* becomes more prominently localized to the dorsal-anterior cap above the nucleus. From late stage 9 to 10B, *grk*RFP* continues to be found above the nucleus and has a fainter appearance.

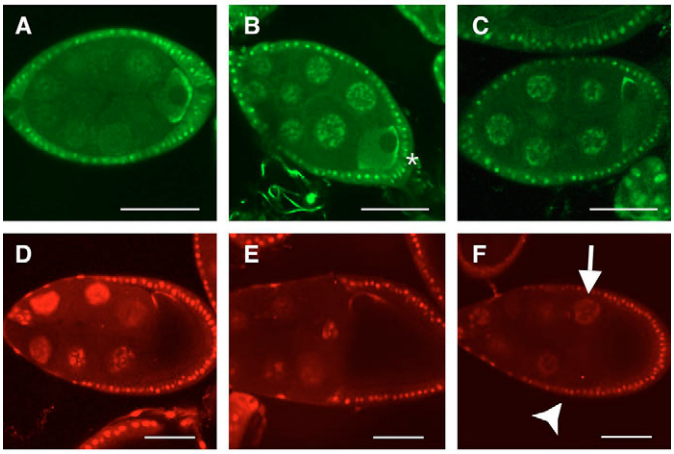


**Fig. 1.** Live imaging of endogenous *grk* mRNA. (A-C) *grk*GFP* expressed in the younger stages of mid-oogenesis. (A) Stage 7 shows posterior accumulation. (B) In early stage 8, there is often a lateral-cortical lining of *grk*GFP* on the side of the oocyte nucleus (asterisk). (C) During late 8, there is no longer a posterior lining of *grk*GFP* but instead the beginnings of an anterior ring with significant accumulation at the ventral anterior. (D,E) *grk*RFP* expressed in older stages of mid-oogenesis. From stages 9 to 10, there is a prominent dorsal-anterior cap and a strong reduction of *grk*RFP* at the ventral-anterior corner. (F) Control line expressing *MCP-RFP* alone. MCP-GFP and MCP-RFP have a nuclear localization sequence, and, as a consequence, when no *grk* mRNA with stem loops is present, the protein will enter the follicle cell nuclei (arrowhead) and nurse cell nuclei (arrow). Bars, 50 μm.

### Actin-destabilizing drugs do not disrupt the maintenance of localized *grk* mRNA in live egg chambers

An intact actin cytoskeleton has been shown to be important for asymmetric localization of RNA and protein in *Drosophila* oocytes (reviewed by Hudson and Cooley, 2002). Treatment with actin-destabilizing drugs, such as cytochalasin D, disrupts the anchoring of *nanos* and *bicoid* mRNA (Forrest and Gavis, 2003; Weil et al., 2006). Also, elimination or reduction of actin-binding proteins, such as moesin and tropomyosin, disrupts the posterior maintenance of Osk protein and mRNA (Jankovics et al., 2002; Polesello et al., 2002). In order to investigate whether *grk* mRNA requires an intact actin framework, we treated live egg chambers expressing *grk*RFP* with the actin-destabilizing drugs latrunculin A and cytochalasin D, either individually or in combination. To test the effectiveness of these drugs, we stained egg chambers with phalloidin, which revealed very reduced, barely detectable F-actin, except for prominent ring canals. The drug concentrations that we used were capable of blocking nurse cell dumping, which results from actin-dependent contractions of the nurse cells (Gutzeit, 1982). Time-lapse imaging of egg chambers from drug-treated GFP-actin flies show rapid depolymerization. We were therefore confident that actin was severely disrupted. Interestingly, we found that *grk*RFP* is well maintained during stages 6-10 (Fig. 2). *grk*RFP* remains tightly anchored both early at the posterior and later at the dorsal-anterior corner, and this anchoring is disrupted only when the drug

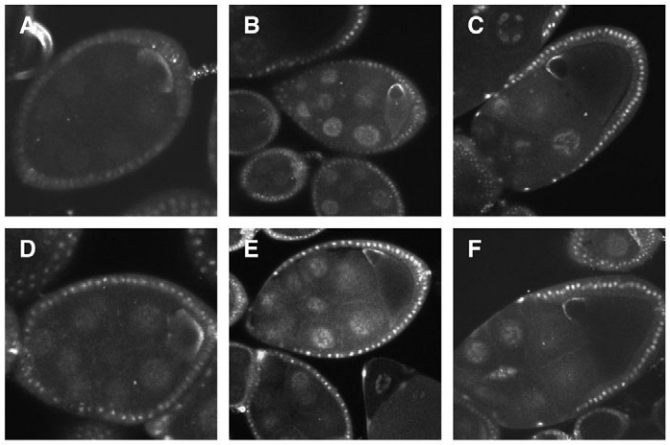


**Fig. 2.** Actin is not necessary for anchorage of *grk* mRNA. (A-C) Dissected live *grk*RFP* egg chambers treated with DMSO, the solent used to dissolve the actin-destabilizing drugs. *grk*RFP* is localized properly from young to late stages. (D-F) Egg chambers were treated with the actin-destabilizing drugs cytochalasin D and latrunculin A for 45-60 minutes. There is no obvious disruption of *grk*RFP*.

concentrations are high enough to cause the oocyte to collapse. In these cases, *grk*RFP* spreads along the cortex of the oocyte. Additionally, we fed adult female *grk*RFP* flies latrunculin A and cytochalasin D and observed that *grk*RFP* was properly localized (data not shown). Similarly, Saunders and Cohen (Saunders and Cohen, 1999) saw no changes in the localization of the *grk* transcript from flies fed cytochalasin D.

### Resistant microtubules might explain why *grk* mRNA remains localized after using microtubule-destabilizing drugs

Microtubules are central for the localization of several mRNAs in *Drosophila* oocytes (St Johnston, 2005). With respect to maintenance, disruption of microtubules has been shown to release *bicoid*, *fs(1)K10*, *orb* and *Bicaudal-D* from the anterior of the oocyte (Pokrywka and Stephenson, 1995). In order to investigate whether an intact microtubule network is needed to maintain *grk* mRNA localization, we treated live egg chambers from flies expressing *grk*RFP* with a combination of the microtubule-destabilizing drugs colchicine and colcemid. After drug treatments, *grk*RFP* localization appeared not to have been disrupted, whether positioned at the posterior or at the dorsal anterior corner during stages 6-10 (Fig. 3). Time-lapse imaging of drug-treated egg chambers over intervals of 45-60 minutes confirmed these results. These results suggest that anchoring of *grk*RFP* is not dependent on microtubules or that the anchoring is meditated by a population of microtubules that are resistant to these inhibitors. To ensure that certain populations of microtubules were indeed disrupted, we monitored the microtubule-dependent ooplasmic streaming that occurs before nurse cell dumping (Gutzeit, 1982). This unidirectional flow ceased within 3 minutes of applying our treatment of colcemid and colchicine, indicating that the drug treatment was very efficient at disrupting microtubules that promote cytoplasmic streaming. We also imaged drug-treated tau-GFP-expressing fly egg chambers. Tau-GFP decorates microtubules and allowed us to follow depolymerization in real time. Interestingly, while depolymerization of microtubules in the oocyte and nurse cells was plainly evident, the microtubule basket surrounding the oocyte nucleus [previously reported at stage 9 by MacDougall and colleagues (MacDougall et al., 2003)] was clearly resistant to the combined effects of colchicine and colcemid (see supplementary material Movie 1). This suggests that there might be different types of microtubules present in the oocyte that have different sensitivities to depolymerizing drugs. Whether *grk*RFP* is anchored to these resistant microtubules is unclear, but our data clearly show that *grk*RFP* is not disrupted by the treatment.

We also examined the combined effect of colcemid and colchicine on *grk*RFP* in egg chambers from females fed with these inhibitors. We observed a range of defects, including loss of *grk*RFP*, mislocalized *grk*RFP* in the oocyte and accumulation of *grk*RFP* in the nurse cells (supplementary material Fig. S1). By contrast, it has been reported that there is an accumulation of *grk* transcripts in the oocytes rather than the nurse cells from colchicine-fed flies (Saunders and Cohen, 1999). The combination of two inhibitors used in our experiments might account for the differences. Nevertheless, under these conditions, it is difficult to distinguish between the roles microtubules might play in mRNA transport versus anchoring within the oocyte.

### *grk* mRNA is a dynamic molecule

In some cases, mRNAs are stably anchored at their destinations. For example, *nanos* mRNA diffuses to the posterior of the oocyte and becomes stably anchored in an actin-dependent manner (Forrest and Gavis, 2003). Dynein acts as a static anchor for the apical transcripts *runt* and *fushi tarazu* in *Drosophila* blastoderm embryos (Delanoue and Davis, 2005). However, recent work indicates that the maintenance of localized mRNAs might also be a dynamic process. *bicoid* mRNA is maintained at the anterior oocyte cortex by continual active transport on microtubules (Weil et al., 2006). To examine whether *grk* mRNA is stably anchored during different stages of oogenesis, we performed FRAP experiments. *grk*GFP* was photobleached, either in the region posterior to the oocyte nucleus during stages 6 and 7 or on the dorsal-lateral side of the cap above the oocyte nucleus during stages 8 and 9 (see supplementary material Movies 2-4). Our FRAP conditions cause photobleaching of a 2.5 $\mu m^2$ area of *grk*GFP* in the focal plane, as well as *grk*GFP* as far out of focus as 2-3 μm above and below

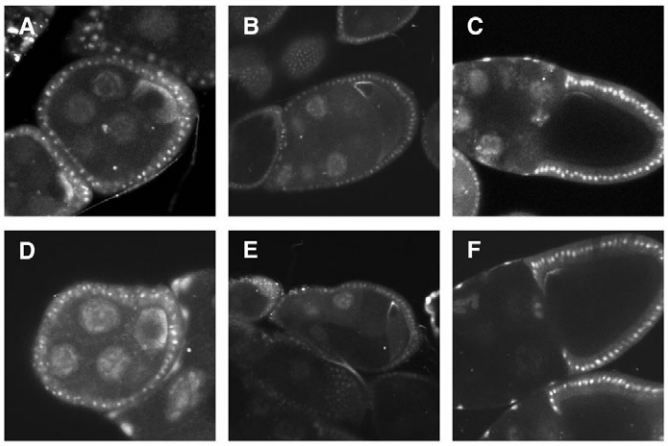


**Fig. 3.** *grk*RFP* appears to remain unaltered after treatment with microtubule-destabilizing drugs. (A-C) Dissected live *grk*RFP* egg chambers treated with ethanol show properly maintained *grk*RFP*. (D-F) Egg chambers were treated with the microtubule-destabilizing drugs colchicine and colcemid for 45-60 minutes. *grk*RFP* does not appear to be disrupted in either young or older egg chambers.

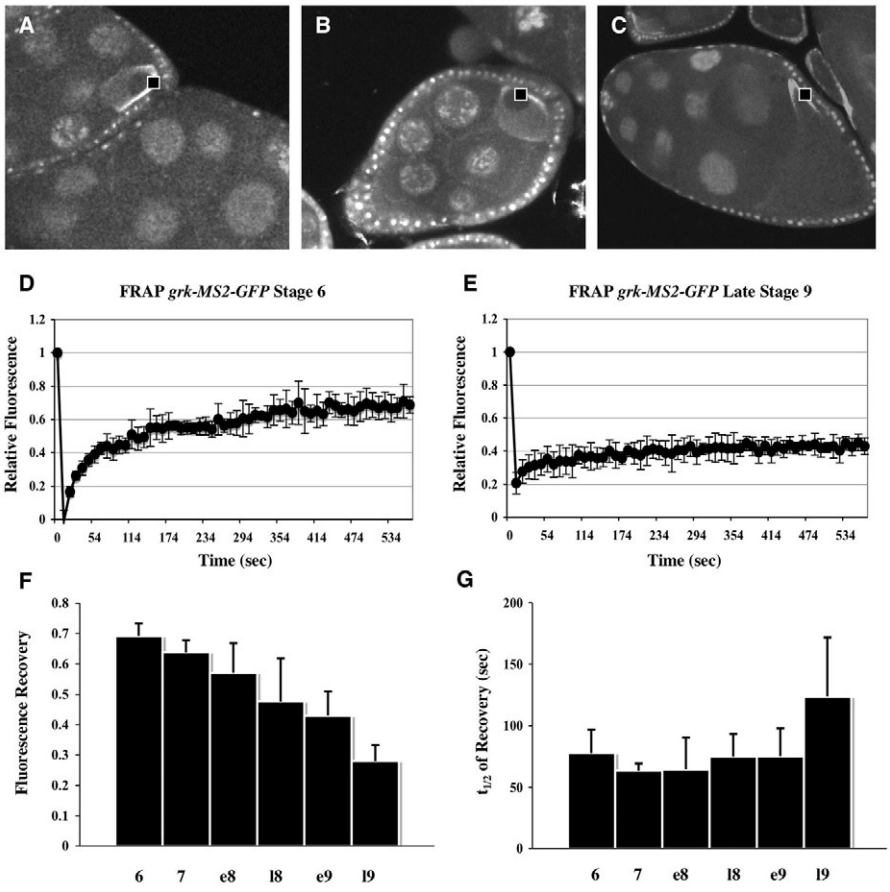


**Fig. 4.** *grk* mRNA is a dynamic molecule. FRAP experiments were performed on *grk*GFP* egg chambers at stages 6-9. (A-C) Images of *grk*GFP* egg chambers at stages 6-9, with a small box representing the area that is bleached during a FRAP experiment. (D,E) Line graphs representing the average relative fluorescence of *grk*GFP* during several FRAP experiments. (D) During stage 6, a defined area of fluorescent *grk*GFP* at the oocyte posterior was bleached and about 70% was recovered. (E) *grk*GFP* localized at the dorsal-anterior cap during late stage 9 was bleached and showed reduced recovery. (F) Bar graph representing the percentage of fluorescence recovery from stages 6 to late stage 9. There is a steady decrease in the amount of recovery as the oocyte progresses through development. (G) Bar graph representing the half-time of recovery ($t_{1/2}$) for stages 6 to late 9. Although recovery steadily decreased, the rate did not, suggesting there could be a similar mechanism occurring during stages 6 to early 9. A minimum of five FRAP experiments were performed for each data point. Bars represent the standard deviation; e, early; l, late.

this plane (supplementary material Fig. S2D-F). Quantitative analysis shows 70% recovery of fluorescence, with a half-time of ~80 seconds ($t_{1/2}=\tau*\ln 2$, where $\tau$ is the time constant of recovery) during stage 6. By contrast, by late stage 9, recovery is reduced to 30%, with a $t_{1/2}$ of >120 seconds (Fig. 4). Thus, the steady-state population of *grk*GFP* is highly dynamic during early stages of oogenesis, but this dynamic behavior subsides at later stages.

What is the source of fluorescence recovery shown by *grk* mRNA? Fluorescence recovery could result from lateral movement of *grk*GFP* that is already localized. To address this possibility, we measured the fluorescence intensity values of the neighboring pools of localized non-bleached *grk*GFP* that surround the bleached area during a FRAP experiment for a corresponding decrease in fluorescence. The fluorescence of these neighboring regions was not decreased, however, implying that recovery does not primarily involve prelocalized sources of *grk*GFP* present at the cortex (Fig. 5). In addition, we performed inverse FRAP experiments on posterior localized *grk*GFP*. We bleached two areas of cortical *grk*GFP* and measured the fluorescence intensity of the localized, non-bleached *grk*GFP* in between the two bleached spots. In these cases, there was no appreciable loss of fluorescence to the non-bleached localized *grk*GFP*, while high fluorescence recovery occurred within the neighboring bleached spots (data not shown). Unless constant and rapid accumulation of new cytoplasmic *grk*GFP* obscures the fluorescence loss from the cortex, our results indicate that the recovery of fluorescence is due to movement of *grk*GFP* from the cytoplasm to the cortex. To determine whether our fast fluorescent recovery is due to newly synthesized *grk*GFP* from the nurse cells, we bleached the entire oocyte at stage 7. We observed partial *grk*GFP* recovery within 20 minutes, more than ten times longer than the recovery observed after bleaching the cortex only (data not shown). Thus, we conclude that, at stage 7, mRNA newly transported from the nurse cells cannot be the major source of cortical recovery and, instead, recovery most probably reflects exchange from the nearby cytoplasm.

### Mislocalized *grk* mRNA in *K10* and *sqd*$^{1}$ mutant oocytes is dynamic

We considered the possibility that mislocalized *grk*GFP* in mutant backgrounds could manifest altered dynamics. In *K10* and *sqd*$^{1}$ mutants (Kelley, 1993; Wieschaus, 1978), *grk* mRNA appears to have normal localization patterns during younger stages of oogenesis, but, in mid-to-late stages, *grk* mRNA is mislocalized along the entire anterior circumference of the oocyte instead of being restricted to the dorsal-anterior corner (Neuman-Silberberg and Schupbach, 1993). In addition, in these mutants, *grk* mRNA is translated along the anterior cortex, resulting in ectopic EGFR activation. Excess receptor activation results in the induction of more dorsal cell fates, leading to expanded dorsal appendages on the egg (Kelley, 1993; Neuman-Silberberg and Schupbach, 1993; Neuman-Silberberg and Schupbach, 1994; Norvell et al., 1999). *grk*GFP* reproducibly shows a similar pattern of localization in either *K10* or *sqd*$^{1}$ mutant backgrounds (Fig. 6B-D).

To examine the behavior of localized and mislocalized *grk* mRNA in the *K10* and *sqd*$^{1}$ mutant oocytes, we performed FRAP experiments. We photobleached the dorsal and ventral anterior corners of *K10* and *sqd*$^{1}$ oocytes (Fig. 6D-F; supplementary material Fig. S3). Interestingly, in mid-to-late stage 9 egg chambers, we found

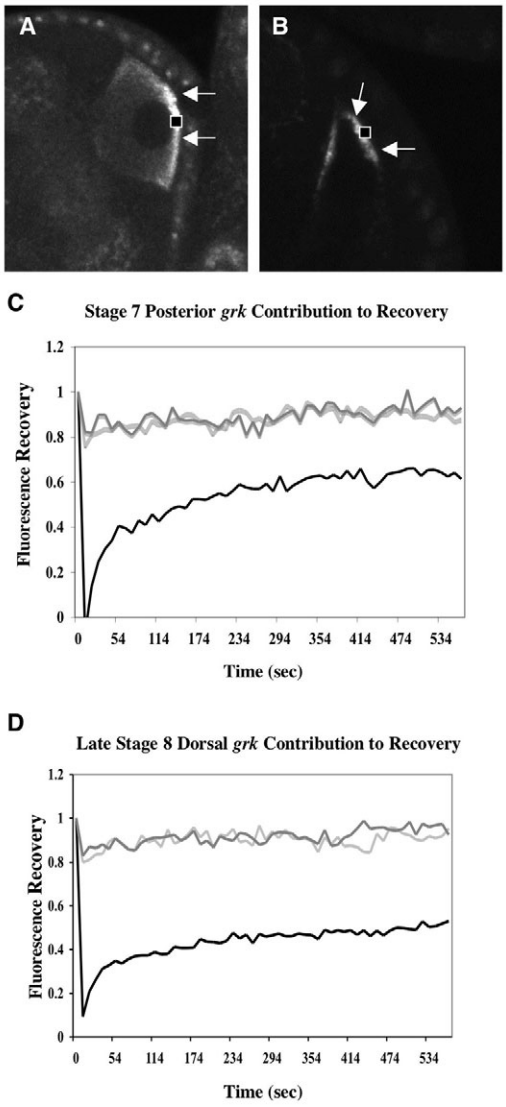


**Fig. 5.** *grk* mRNA recovery does not specifically involve depletion of nearby localized sources. (A,B) Images of stage 7 (A) and late stage 8 (B) egg chambers from flies expressing *grk*GFP* illustrating the region bleached during the FRAP experiment (black box), plus arrows pointing to the unbleached areas of *grk*GFP* monitored for fluorescence loss. (C,D) Line graphs representing average relative fluorescence of *grk*GFP* and two unbleached neighboring pools of *grk*GFP* during FRAP experiments. In panel C, the two posterior pools that surrounded the bleached region of *grk*GFP* during stage 7 show no dramatic decrease in fluorescence intensity. The pool on the right of the bleached region is represented by the dark gray line, whereas the pool on the left is the pale gray line. (D) Likewise, the surrounding sources of localized *grk*GFP* found at the dorsal-anterior cap during late stage 8 also displayed no measurable decrease while recovery occurred (right, dark gray; left, pale gray). This suggests that recovery is not due to nearby localized sources of *grk*GFP*.

*grk*GFP* at both the dorsal and ventral sides to be dynamic. In fact, *grk*GFP* is more dynamic (~45% recovery) compared with *grk*GFP* in a wild-type background (~25%) at this stage (Fig. 6E and supplementary material Movie 5). Accordingly, the recovery rates ($t_{1/2}$) for *grk*GFP* during mid-to-late stage 9 egg chambers in the mutant backgrounds are much faster. The nature of *grk*GFP* dynamics resembles that of a younger stage with faster and higher recovery, significantly different from the control, which displayed a slow rate with little recovery (Fig. 6F). We also performed FRAP experiments on *K10* and *sqd*$^{1}$ mutants at stages 6 and 7, when *grk* mRNA is properly localized at the posterior (supplementary material Fig. S4). Surprisingly, we found a substantial amount of variability in *K10* mutants and a general increase of recovery in *sqd*$^{1}$ mutants.

### Compromised dynein activity interferes with the recovery of *grk* mRNA

Recent evidence for direct binding between *grk* mRNA and the dynein light chain adds to the mounting support for the potential role of the dynein motor enzyme in *grk* mRNA localization (Rom et al., 2007). Given the dynamic nature of *grk* mRNA, we examined the behavior of *grk*GFP* under conditions that compromise dynein motor activity. First, we overexpressed dynamitin (Dmn), which is an essential component of the dynactin complex and is necessary for dynein activity (Kamal and Goldstein, 2002). Overexpression of Dmn results in an increase of anteriorly localized *grk* mRNA during mid-stages of oogenesis, as seen by in situ hybridization, and mispositioning of the oocyte nucleus (Duncan and Warrior, 2002; Januschke et al., 2002). Second, we took advantage of hypomorphic dynein heavy chain alleles (*dhc*) alleles, which permit oogenesis but have been shown to reduce transport (Clark et al., 2007; Weil et al., 2006).

FRAP experiments were performed on localized *grk*GFP* in oocytes where dynein function was reduced by either of the above methods. In both situations, we observed mislocalized *grk*GFP* in the oocyte cytoplasm accompanied by large aggregates, from stages 5 to 10. These large aggregates are most clearly visible in the nurse cell cytoplasm and are very reminiscent of the aggregates we observed in colchicine-fed *grk*GFP* flies (supplementary material Fig. S1B). Upon overexpression of Dmn, a significant portion of *grk*GFP* is still capable of reaching its proper destination, both at the posterior and dorsal-anterior corner (Fig. 7C,D). In *dhc*$^{6\text{-}10/6\text{-}12}$ egg chambers (Fig. 7E,F), *grk*GFP* no longer accumulates in a thin crescent along the posterior cortex during stages 6 and 7 and instead is very diffuse throughout the oocyte. During mid-stages of oogenesis, there is an accumulation of *grk*GFP* at the anterior cortex beginning as early as stage 7. A defined area of fluorescent *grk* mRNA at the posterior and dorsal-anterior was bleached during FRAP experiments. With overexpression of Dmn, fluorescence recovery is reduced to 34% in stages 6-7 and 28% in stage late 8 to early 9 (l8-e9). Similarly, in dynein mutant egg chambers, *grk*GFP* recovery is reduced to 24% at stage l8-9. This is in direct contrast to control fluorescence recovery values of 67% for stages 6-7 and 46% for l8-e9 stages (Fig. 7G). Taken together, our results show that, when dynein is compromised by two different methods, we observe a significant reduction in the dynamics of *grk* mRNA.

## Discussion

In order to visualize *grk* mRNA in vivo, we used the MS2-MCP system. Unlike in situ hybridization or FISH techniques that reveal static images of RNA, the MS2-MCP system has allowed us to observe live samples and film *grk* mRNA during various stages of oogenesis. Using this new detection method, we have described the live localization patterns of fluorescent *grk* mRNA. Our description is similar to those originally published (Neuman-Silberberg and Schupbach, 1993) and confirms observations recently published using FISH (MacDougall et al., 2003). We also describe *grk* mRNA accumulating at the anterior before the posterior localization has

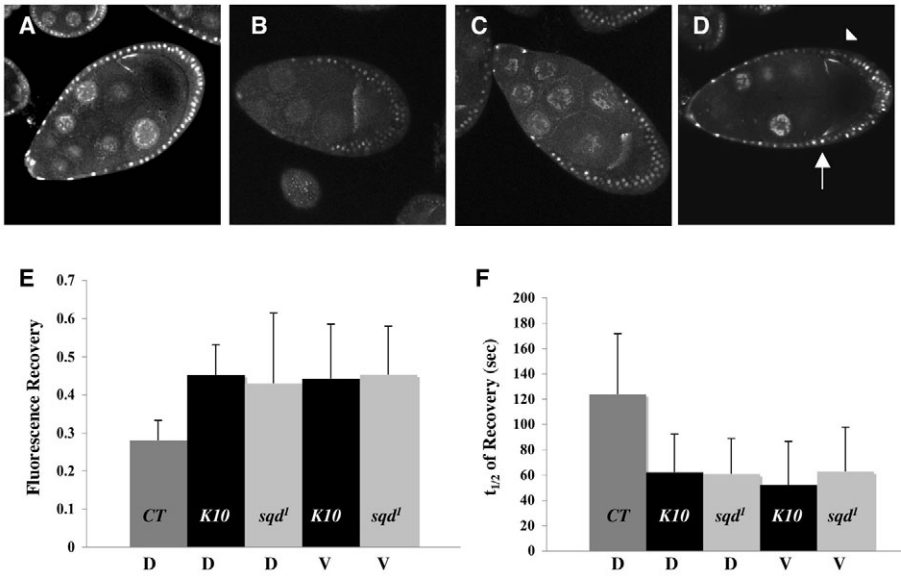


**Fig. 6.** Mislocalized *grk* mRNA at the anterior is dynamic. FRAP experiments were performed on *K10; grk*GFP* and *grk*GFP; sqd*$^{1}$ egg chambers. Images of *grk*GFP* (A), *K10; grk*GFP* (B,D) and *grk*GFP; sqd*$^{1}$ (C) egg chambers during mid-to-late stage 9. (B-D) Mislocalized *grk*GFP* forms an anterior ring at the edge of the oocyte. A defined area of fluorescent *grk* mRNA at the dorsal (arrowhead) and ventral-anterior (arrow) sides was bleached during FRAP experiments. (E) Previously we noted that *grk*GFP* localized at the dorsal-anterior cap during mid-to-late stage 9 had very reduced recovery (~25% recovery) during FRAP experiments. By contrast, *grk*GFP* found both at the dorsal and ventral-anterior sides of *K10* and *sqd*$^{1}$ mutants was more dynamic (~45%). (F) Bar graph representing the half-time of recovery ($t_{1/2}$) for *grk*GFP* during mid-to-late stage 9 from controls and mutant lines. Recovery rates are much faster in the mutants, similar to the younger stages in the control line (Fig. 4). A minimum of five FRAP experiments were taken for each data point. Error bars represent standard deviations.

disappeared. Moreover, in early stage 8, we observe a lateral accumulation of *grk* mRNA that persists on the side of the oocyte where the nucleus is found (the future dorsal side), whereas, at the same time, the opposite side (the future ventral side) no longer has *grk* mRNA except for a small accumulation at the anterior cortex. At this transitional stage, large amounts of *grk* mRNA line the entire anterior and dorsal cortex of the oocyte. This configuration eventually resolves to the well-defined dorsal-anterior cap, by first restricting *grk* mRNA on the dorsal side, followed by restricting *grk* mRNA at the anterior. The question arises as to whether *grk* mRNA is transported along the lateral wall from the posterior to the dorsal-anterior corner or whether the lateral RNA decays and new *grk* mRNA transcripts populate the corner from the nurse cells. As endogenous *grk* mRNA does not form particles large enough to be resolved and tracked with our imaging system, we are presently unable to address this question. Using photoswitchable fluorescent molecules in combination with the MS2-MCP system could provide some answers to these questions in the future.

The process of RNA localization is likely to involve several of the following steps: RNP assembly, nuclear export, cytoplasmic transport, anchorage, translation and decay (St Johnston, 2005). Stable anchorage versus continuous transport have been proposed as two different mechanisms for the maintenance of mRNAs before translation occurs. Possible anchors can be microfilaments, microtubules, proteins and even noncoding RNAs, such as the Xlsirts in *Xenopus* oocytes (Kloc and Etkin, 2005). Continuous transport can give the appearance of an mRNA having a static anchor because this dynamic mechanism can result in a net gain of accumulation. In fact, *bicoid* mRNA has recently been shown to be maintained in late oocytes by continual active transport (Weil et al., 2006). Unexpectedly, it has been demonstrated that dynein, separate from its motor function, can act as a static anchor for apical transcripts in *Drosophila* embryos (Delanoue and Davis, 2005). In an attempt to study whether the cytoskeleton is a necessary factor for the maintenance of already localized *grk* transcripts, we used cytoskeleton-destabilizing drugs. Our results suggest that actin does not play a role in the anchorage. This also corresponds to data obtained by moesin-deficient flies, which have defects in localization of *oskar* mRNA because of a loose and detached actin network, but in which *grk* mRNA remains undisrupted (Jankovics et al., 2002; Polesello et al., 2002). Interestingly however, Babu and colleagues (Babu et al., 2004) showed that *osk* mRNA has two redundant anchoring processes. They noted that latrunculin A treatments did not disrupt the maintenance of *osk* unless other proteins, such as Homer, were absent (Babu et al., 2004). It is therefore possible that the actin cytoskeleton is similarly involved in the maintenance of *grk* mRNA in a manner redundant with that of other proteins, but so far no actin-binding proteins have been found to bind directly to the *grk* mRNA.

Using microtubule-destabilizing drugs, we see no obvious disruption of localized *grk* mRNA throughout stages 6-10. This agrees with injection studies using *grk* mRNA synthesized in vitro that show that show localized *grk* mRNA is not disrupted by the later injection of colcemid (MacDougall et al., 2003). Interestingly, we observed that the microtubule network around the oocyte nucleus of stage 9-10 egg chambers was resistant to our drug treatments. It is not uncommon to observe populations of microtubules to be resistant to depolymerizing drugs. Often it is a characteristic of stable versus dynamic populations of microtubules (Baas et al., 1994; Bannigan et al., 2006; Guillaud et al., 1998; Palazzo et al., 2003). These microtubules persist even when nuclear migration is disrupted in *grk* mutants, or when the nucleus is displaced in various other mutants (Guichet et al., 2001; Januschke et al., 2002). It is possible that *grk* mRNA might attach itself to these MTs. Moreover, overexpressing Dmn, a component of the dynein-dynactin complex, disrupts this oocyte nucleus microtubule scaffold, resulting in *grk* mRNA being dispersed in the oocyte within stage 10 egg chambers (Januschke et al., 2002), very similar to what we saw in our experiments. During stages 9 and 10, when we observed the resistant microtubule basket, our FRAP studies show little fluorescence recovery. During these later stages, *grk* mRNA therefore appears to have a more stable anchorage and might no longer be in transit, whereas the high percentage and fast rate of recovery during younger stages suggests a high transport phase. The $t_{1/2}$ is remarkably similar for stages 6 to early 9, suggesting a similar mechanism might be occurring during these stages. However, recovery slows down at mid-to-late stage 9 and is likely to be indicative of a shift in an equilibrium to a more stably anchored *grk* mRNA. Recovery does

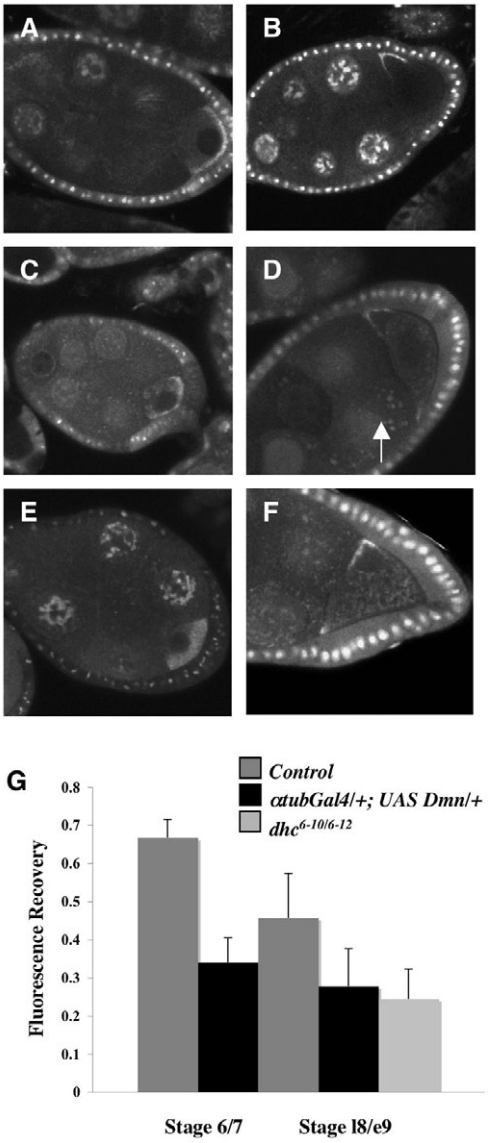


**Fig. 7.** Reducing dynein activity leads to reduced *grk* mRNA recovery. FRAP experiments were performed on *grk*GFP; αtubGal4/+;UAS-Dmn/+* and *grk*GFP; dhc*$^{6\text{-}10/6\text{-}12}$ egg chambers. Images of *grk*GFP* (A,B), *grk*GFP; αtubGal4/+;UAS-Dmn/+* egg (C,D) and *grk*GFP; dhc*$^{6\text{-}10/6\text{-}12}$ (E,F) egg chambers during stages 6-7 (A,C,E) and late 8 to early 9 (B,D,F). (A,B) Properly localized *grk*GFP* lines the posterior cortex of young egg chambers, whereas *grk*GFP* forms a crescent around the oocyte nucleus at the dorsal anterior corner starting stage 8. In a UAS-Dmn background (C,D), there is mislocalized *grk*GFP* in the oocyte cytoplasm accompanied by large aggregates that can also be seen in the nurse cells (arrow). Under these conditions, a significant proportion of *grk*GFP* is capable of reaching its destination both at the posterior and dorsal-anterior corner. In hypomorphic alleles (E,F), *grk*GFP* has a very diffuse localization during young stages and accumulates at the anterior cortex in later stages. Similar to (C,D), there are aggregates in both the nurse cell and oocyte cytoplasm. A defined area of fluorescent *grk* at the posterior and dorsal-anterior was bleached during FRAP experiments. (G) In control early stages (6-7), *grk*GFP* has on average 67% fluorescence recovery and during mid-stages (l8 to e9) a 46% recovery during FRAP experiments, whereas by contrast a significant reduction occurs in both young and mid stages when dynein activity is compromised. When Dmn is overexpressed, recovery is reduced to 34% in stages 6-7 and 28% in l8-e9. Similarly, in the dynein hypomorphs, recovery is reduced to 24% in stage l8-e9 egg chambers. A minimum of five FRAP experiments were performed for each data point. Error bars represent standard deviations.

not appear to be from prelocalized sources of *grk* mRNA. It appears to occur instead from nearby cytoplasm. At least at stage 7, the recovery is not due to nurse cells. At later stages, the low amount of recovery could represent *grk* mRNA in transit from the nurse cells (already close to its destination) (Clark et al., 2007) or this could also be explained by continual active transport. Further studies are needed to distinguish between these possibilities.

The difference in dynamics of *grk* mRNA between young and old oocytes is altered in *K10* and *sqd*$^{1}$ mutants. In fact, during the later stages, we found an increase in recovery in the mutants, suggesting the existence of a more dynamic *grk* mRNA at the anterior of the oocytes. The rate of recovery also does not slow down and is more representative of *grk* mRNA in a younger oocyte. It might be that, in addition to a defect in the machinery needed for proper localization (Norvell et al., 1999), the transition to a more stable anchorage is impaired in these mutants. In fact, in a recent publication, Delanoue and colleagues (Delanoue et al., 2007) suggest that Squid is a necessary component for the conversion of *grk* transport particles to a more stable structure. In addition, we found that compromising the activity of dynein by either overexpressing Dmn or using hypomorphic alleles of the dynein heavy chain led to less fluorescence recovery in both young and mid stages. Although we could not directly distinguish the roles of dynein in either long-range transport or anchorage, we have demonstrated that, when dynein activity is reduced, localized *grk* mRNA is less dynamic.

Using the MS2-MCP system, we have been able to visualize *grk* mRNA in live egg chambers and have begun to dissect the processes involved in the maintenance of localized transcripts. We show that *grk* mRNA has a remarkably different set of dynamics between young and older egg chambers and we also measured differences in various mutant backgrounds, which allows us to define the various stages involved in the process.

## Materials and Methods

### *Drosophila* stocks

*hsp83-MCP-RFP* and *hsp83-MCP-GFP* transgenic flies have been described previously (Forrest and Gavis, 2003; Weil et al., 2006). We used *fs(1)K10*, *sqd*$^{1}$, *dhc*$^{6-10}$ and *dhc*$^{6-12}$ mutant strains (Kelley, 1993; Li et al., 1994; Wieschaus, 1978). Antoine Guichet provided the UAS-Dmn flies (Guichet et al., 2001). Overexpression of Dmn was achieved by using the *αtubGal4* driver that begins to be active during stage 4 (*matαGal4-67*). For marker mutations, Gal4 lines and balancer chromosomes, see flybase@indiana.edu.

### Transgene construction

A *Pml*I site was introduced at 1603 bp of the mRNA, within the 3′UTR of *grk* mRNA. This site is 343 bp after the stop codon. The mutagenesis was performed on a 5050 bp genomic fragment containing the complete *grk* locus (Queenan et al., 1999) with adjacent 5′ and 3′ sequences within the pBluescript II SK+ phagemid (Stratagene). The pSL-MS2-12 construct contains 12 MS2 stem loops (a gift from K. Forrest). We used a mutated version of the stem loop that results in a very strong affinity ($K_d$=$10^{-11}$) of MS2 coat protein to the MS2 stem loop (Johansson et al., 1998; Valegard et al., 1997). The 693 bp *Bam*HI-*Eco*RV fragment from pSL-MS2-12 was end-filled with klenow (NE Biolabs) and placed into the *Pml*I site of *grk*. A XhoI-EagI *grk*-MS2-12 fragment was cloned into pCasper4 using *Xho*I-*Not*I.

### P-element-mediated transformation

P-element transformation was performed according to standard procedures (Spradling and Rubin, 1982) using an Eppendorf Transjector 5246 with Eppendorf Femtotips (Eppendorf). Transgene constructs were injected at a concentration of 0.4 μg/μl along with the helper plasmid pTurbo at a concentration of 0.1 μg/μl.

### Live imaging and inhibitor treatment

Ovaries were dissected in Schneider's *Drosophila* Medium (Gibco). Egg chambers were placed in No. 1.5 glass-bottom culture dishes (MatTek) with 200 μl of medium. A No. 1.5 micro cover glass (VWR) was cut with a diamond tip to a coverslip of about 4 mm$^2$ and placed on top of the dissected egg chambers. Egg chambers were treated with either 200 μg/ml colchicine and 100 μg/ml colcemid (Sigma) or 4.2

μg/ml latrunculin A and 100 μg/ml cytochalasin D (Sigma) for 45-65 minutes while in the glass-bottom dishes.

### FRAP experiments

FRAP experiments were performed using a Zeiss LSM510 confocal microscope with a 40 1.2 NA water objective lens. Imaging was performed with a 488 nm argon laser. The following conditions gave minimal photobleaching: 70% laser output, 1.5% AOTF, zoom 4, scan speed 6, 10 seconds per frame. For each FRAP experiment, 1-3 pre-bleach images were taken. A defined region of interest (ROI), a 2.25 $\mu m^2$ region, was bleached at 80% power with 15 iterations (~4 seconds). After bleaching, a time series was taken every 10 seconds for a total of 10 minutes. Analysis was done using MATLAB and ImageJ (NIH). In order to test for the survival and transport properties of the egg chamber, we bleached the entire oocyte of stage 8 *GFP-Spn-F* egg chambers (Abdu et al., 2006) and monitored the recovery of Spn-F protein for 20 minutes. GFP-Spn-F is transported from nurse cells to the oocyte and, under our experimental conditions, significant recovery occurs (data not shown).

### Feeding inhibitor drugs

Flies were starved for 24 hours. After starvation, the flies were placed in a vial for 24 hours containing fly food media topped with a coated layer of yeast and inhibitor drugs (200 μg/ml colchicine and 100 μg/ml colcemid or 4.2 μg/ml latrunculin A and 100 μg/ml cytochalasin D). Ovaries were then dissected and fixed with 4% paraformaldehyde.

We thank Kevin Forrest for technical advice and reagents, Thomas Gregor for help with MATLAB analysis and Antoine Guichet for flies. We also thank the members of the Wieschaus and Schupbach labs for their insightful critiques of the work involved in the manuscript. This work was supported by the Howard Hughes Medical Institute (A.M.J. and T.S.) and by a grant from the National Institutes of Health (GM067758) to E.R.G.

## References

**Abdu, U., Bar, D. and Schupbach, T.** (2006). spn-F encodes a novel protein that affects oocyte patterning and bristle morphology in Drosophila. *Development* **133**, 1477-1484.

**Baas, P. W., Pienkowski, T. P., Cimbalnik, K. A., Toyama, K., Bakalis, S., Ahmad, F. J. and Kosik, K. S.** (1994). Tau confers drug stability but not cold stability to microtubules in living cells. *J. Cell Sci.* **107**, 135-143.

**Babu, K., Cai, Y., Bahri, S., Yang, X. and Chia, W.** (2004). Roles of Bifocal, Homer, and F-actin in anchoring Oskar to the posterior cortex of Drosophila oocytes. *Genes Dev.* **18**, 138-143.

**Bannigan, A., Wiedemeier, A. M., Williamson, R. E., Overall, R. L. and Baskin, T. I.** (2006). Cortical microtubule arrays lose uniform alignment between cells and are oryzalin resistant in the Arabidopsis mutant, radially swollen 6. *Plant Cell Physiol.* **47**, 949-958.

**Berleth, T., Burri, M., Thoma, G., Bopp, D., Richstein, S., Frigerio, G., Noll, M. and Nusslein-Volhard, C.** (1988). The role of localization of bicoid RNA in organizing the anterior pattern of the Drosophila embryo. *EMBO J.* **7**, 1749-1756.

**Bertrand, E., Chartrand, P., Schaefer, M., Shenoy, S. M., Singer, R. H. and Long, R. M.** (1998). Localization of ASH1 mRNA particles in living yeast. *Mol. Cell* **2**, 437-445.

**Brendza, R. P., Serbus, L. R., Saxton, W. M. and Duffy, J. B.** (2002). Posterior localization of dynein and dorsal-ventral axis formation depend on kinesin in Drosophila oocytes. *Curr. Biol.* **12**, 1541-1545.

**Clark, A., Meignin, C. and Davis, I.** (2007). A Dynein-dependent shortcut rapidly delivers axis determination transcripts into the Drosophila oocyte. *Development* **134**, 1955-1965.

**Delanoue, R. and Davis, I.** (2005). Dynein anchors its mRNA cargo after apical transport in the Drosophila blastoderm embryo. *Cell* **122**, 97-106.

**Delanoue, R., Herpers, B., Soetaert, J., Davis, I. and Rabouille, C.** (2007). Drosophila Squid/hnRNP helps Dynein switch from a gurken mRNA transport motor to an ultrastructural static anchor in sponge bodies. *Dev. Cell* **13**, 523-538.

**Duncan, J. E. and Warrior, R.** (2002). The cytoplasmic dynein and kinesin motors have interdependent roles in patterning the Drosophila oocyte. *Curr. Biol.* **12**, 1982-1991.

**Ephrussi, A., Dickinson, L. K. and Lehmann, R.** (1991). Oskar organizes the germ plasm and directs localization of the posterior determinant nanos. *Cell* **66**, 37-50.

**Forrest, K. M. and Gavis, E. R.** (2003). Live imaging of endogenous RNA reveals a diffusion and entrapment mechanism for nanos mRNA localization in Drosophila. *Curr. Biol.* **13**, 1159-1168.

**Goodrich, J. S., Clouse, K. N. and Schupbach, T.** (2004). Hrb27C, Sqd and Otu cooperatively regulate gurken RNA localization and mediate nurse cell chromosome dispersion in Drosophila oogenesis. *Development* **131**, 1949-1958.

**Guichet, A., Peri, F. and Roth, S.** (2001). Stable anterior anchoring of the oocyte nucleus is required to establish dorsoventral polarity of the Drosophila egg. *Dev. Biol.* **237**, 93-106.

**Guillaud, L., Bosc, C., Fourest-Lieuvin, A., Denarier, E., Pirollet, F., Lafanechere, L. and Job, D.** (1998). STOP proteins are responsible for the high degree of microtubule stabilization observed in neuronal cells. *J. Cell Biol.* **142**, 167-179.

**Gutzeit, H. O.** (1982). Time-lapse film analysis of cytoplasmic streaming during late oogenesis of Drosophila. *J. Embryol. Exp. Morphol.* **67**, 101-111.

**Hudson, A. M. and Cooley, L.** (2002). Understanding the function of actin-binding proteins through genetic analysis of Drosophila oogenesis. *Annu. Rev. Genet.* **36**, 455-488.

**Jankovics, F., Sinka, R., Lukacsovich, T. and Erdelyi, M.** (2002). MOESIN crosslinks actin and cell membrane in Drosophila oocytes and is required for OSKAR anchoring. *Curr. Biol.* **12**, 2060-2065.

**Januschke, J., Gervais, L., Dass, S., Kaltschmidt, J. A., Lopez-Schier, H., St Johnston, D., Brand, A. H., Roth, S. and Guichet, A.** (2002). Polar transport in the Drosophila oocyte requires Dynein and Kinesin I cooperation. *Curr. Biol.* **12**, 1971-1981.

**Johansson, H. E., Dertinger, D., LeCuyer, K. A., Behlen, L. S., Greef, C. H. and Uhlenbeck, O. C.** (1998). A thermodynamic analysis of the sequence-specific binding of RNA by bacteriophage MS2 coat protein. *Proc. Natl. Acad. Sci. USA* **95**, 9244-9249.

**Kamal, A. and Goldstein, L. S.** (2002). Principles of cargo attachment to cytoplasmic motor proteins. *Curr. Opin. Cell Biol.* **14**, 63-68.

**Kelley, R. L.** (1993). Initial organization of the Drosophila dorsoventral axis depends on an RNA-binding protein encoded by the squid gene. *Genes Dev.* **7**, 948-960.

**Kloc, M. and Etkin, L. D.** (2005). RNA localization mechanisms in oocytes. *J. Cell Sci.* **118**, 269-282.

**Lehmann, R. and Nusslein-Volhard, C.** (1986). Abdominal segmentation, pole cell formation, and embryonic polarity require the localized activity of oskar, a maternal gene in Drosophila. *Cell* **47**, 141-152.

**Li, M., McGrail, M., Serr, M. and Hays, T. S.** (1994). Drosophila cytoplasmic dynein, a microtubule motor that is asymmetrically localized in the oocyte. *J. Cell Biol.* **126**, 1475-1494.

**MacDougall, N., Clark, A., MacDougall, E. and Davis, I.** (2003). Drosophila gurken (TGFalpha) mRNA localizes as particles that move within the oocyte in two dynein-dependent steps. *Dev. Cell* **4**, 307-319.

**Manseau, L. J. and Schupbach, T.** (1989). cappuccino and spire: two unique maternal-effect loci required for both the anteroposterior and dorsoventral patterns of the Drosophila embryo. *Genes Dev.* **3**, 1437-1452.

**Neuman-Silberberg, F. S. and Schupbach, T.** (1993). The Drosophila dorsoventral patterning gene gurken produces a dorsally localized RNA and encodes a TGF alpha-like protein. *Cell* **75**, 165-174.

**Neuman-Silberberg, F. S. and Schupbach, T.** (1994). Dorsoventral axis formation in Drosophila depends on the correct dosage of the gene gurken. *Development* **120**, 2457-2463.

**Neuman-Silberberg, F. S. and Schupbach, T.** (1996). The Drosophila TGF-alpha-like protein Gurken: expression and cellular localization during Drosophila oogenesis. *Mech. Dev.* **59**, 105-113.

**Norvell, A., Kelley, R. L., Wehr, K. and Schupbach, T.** (1999). Specific isoforms of squid, a Drosophila hnRNP, perform distinct roles in Gurken localization during oogenesis. *Genes Dev.* **13**, 864-876.

**Palazzo, A., Ackerman, B. and Gundersen, G. G.** (2003). Cell biology: tubulin acetylation and cell motility. *Nature* **421**, 230.

**Pokrywka, N. J. and Stephenson, E. C.** (1995). Microtubules are a general component of mRNA localization systems in Drosophila oocytes. *Dev. Biol.* **167**, 363-370.

**Polesello, C., Delon, I., Valenti, P., Ferrer, P. and Payre, F.** (2002). Dmoesin controls actin-based cell shape and polarity during Drosophila melanogaster oogenesis. *Nat. Cell Biol.* **4**, 782-789.

**Queenan, A. M., Barcelo, G., Van Buskirk, C. and Schupbach, T.** (1999). The transmembrane region of Gurken is not required for biological activity, but is necessary for transport to the oocyte membrane in Drosophila. *Mech. Dev.* **89**, 35-42.

**Rom, I., Faicevici, A., Almog, O. and Neuman-Silberberg, F. S.** (2007). Drosophila Dynein light chain (DDLC1) binds to gurken mRNA and is required for its localization. *Biochim. Biophys. Acta* **1773**, 1526-1533.

**Saunders, C. and Cohen, R. S.** (1999). The role of oocyte transcription, the 5′UTR, and translation repression and derepression in Drosophila gurken mRNA and protein localization. *Mol. Cell* **3**, 43-54.

**Spradling, A. C. and Rubin, G. M.** (1982). Transposition of cloned P elements into Drosophila germ line chromosomes. *Science* **218**, 341-347.

**St Johnston, D.** (2005). Moving messages: the intracellular localization of mRNAs. *Nat. Rev. Mol. Cell Biol.* **6**, 363-375.

**Valegard, K., Murray, J. B., Stonehouse, N. J., van den Worm, S., Stockley, P. G. and Liljas, L.** (1997). The three-dimensional structures of two complexes between recombinant MS2 capsids and RNA operator fragments reveal sequence-specific protein-RNA interactions. *J. Mol. Biol.* **270**, 724-738.

**Van Buskirk, C. and Schupbach, T.** (1999). Versatility in signaling: multiple responses to EGF receptor activation during Drosophila oogenesis. *Trends Cell Biol.* **9**, 1-4.

**Weil, T. T., Forrest, K. M. and Gavis, E. R.** (2006). Localization of bicoid mRNA in late oocytes is maintained by continual active transport. *Dev. Cell* **11**, 251-262.

**Wieschaus, E., Marsh, J. L. and Gehring, W.** (1978). fs(1)K10, a germline-dependent female sterile mutation causing abnormal chorion morphology in Drosophila melanogaster. *Roux's Arch. Dev. Biol.* **184**, 75-82.